



Published in final edited form as:

J Appl Physiol. 2007 May ; 102(5): 1739–1745. doi:10.1152/jappphysiol.00948.2006.

The melting of pulmonary surfactant monolayers

Wenfei Yan, Samares C. Biswas, Ted G. Laderas, and Stephen B. Hall

Departments of Biochemistry & Molecular Biology, Medicine, and Physiology & Pharmacology, Oregon Health & Science University, Portland, Oregon

Abstract

Monomolecular films of phospholipids in the liquid-expanded (LE) phase after supercompression to high surface pressures (π), well above the equilibrium surface pressure (π_e) at which fluid films collapse from the interface to form a three-dimensional bulk phase, and in the tilted-condensed (TC) phase both replicate the resistance to collapse that is characteristic of alveolar films in the lungs. To provide the basis for determining which film is present in the alveolus, we measured the melting characteristics of monolayers containing TC dipalmitoyl phosphatidylcholine (DPPC), as well as supercompressed 1-palmitoyl-2-oleoyl phosphatidylcholine and calf lung surfactant extract (CLSE). Films generated by appropriate manipulations on a captive bubble were heated from $\approx 27^\circ\text{C}$ to $\approx 60^\circ\text{C}$ at different constant π above π_e . DPPC showed the abrupt expansion expected for the TC-LE phase transition, followed by the contraction produced by collapse. Supercompressed CLSE showed no evidence of the TC-LE expansion, arguing that supercompression did not simply convert the mixed lipid film to TC DPPC. For both DPPC and CLSE, the melting point, taken as the temperature at which collapse began, increased at higher π , in contrast to 1-palmitoyl-2-oleoyl phosphatidylcholine, for which higher π produced collapse at lower temperatures. For π between 50 and 65 mN/m, DPPC melted at 48–55°C, well above the main transition for bilayers at 41°C. At each π , CLSE melted at temperatures $>10^\circ\text{C}$ lower. The distinct melting points for TC DPPC and supercompressed CLSE provide the basis by which the nature of the alveolar film might be determined from the temperature-dependence of pulmonary mechanics.

Keywords

captive bubble; dipalmitoyl phosphatidylcholine; jammed; monolayer; pulmonary mechanics; supercompressed

The behavior of pulmonary surfactant indicates that films at the air/water interface in the alveoli are solid. Multiple approaches consistently indicate that, when compressed by the decreasing alveolar surface area during exhalation, the films of pulmonary surfactant reach high surface pressures (π) (13, 19, 30, 35, 37, 39). The observed values are well above the equilibrium spreading pressure (π_e) of ~ 46 mN/m, at which two-dimensional monomolecular films coexist at equilibrium with their three-dimensional bulk phases (14). Films under equilibrium conditions never reach $\pi > \pi_e$, because compression produces only flow of constituents into the bulk phase, with no increase in the density of material within the interface. The $\pi > \pi_e$ observed in static lungs, therefore, indicate that the alveolar films deviate from equilibrium and must by definition be metastable. The rate at which a film flows into the bulk phase in response to the thermodynamic driving force of $(\pi - \pi_e)$ can be

used to calculate an effective viscosity (27). The very slow rates at which films in the lungs undergo this process of collapse from the interface indicate that they have achieved the high viscosities that define a solid (2).

Two kinds of solid films in vitro replicate the slow rates of collapse observed in the lungs. Films in the highly ordered tilted-condensed (TC) phase approach the structure of a two-dimensional crystal (23). Dipalmitoyl phosphatidylcholine (DPPC), which is present in pulmonary surfactant at higher levels than in other biological lipids, can form TC films at physiological temperatures (7, 9). The classical model of pulmonary surfactant contends that the functional film in the alveolus is a TC monolayer of essentially pure DPPC (1, 6). More recent studies have shown that fluid films in the liquid-expanded (LE) phase can also become solid if they reach π sufficiently far above π_c (8, 33). During heating, these films recover fluid characteristics, defined by rapid rates of collapse, with only the same expansion of molecular area that occurs for films of the same material that have not reached high π (36). This observation suggests that the transformation at high π of the initially fluid films to a metastable form occurs without a major structural change, such as a first-order phase transition. The fluid monolayers that are supercompressed to π sufficiently far above π_c , at which they would form the bulk phase under equilibrium conditions, may, therefore, be analogous to the amorphous solids, or glasses, formed by three-dimensional liquids that are supercooled sufficiently far below their freezing points (28, 33). The supercompressed fluid films would then represent another example of a system that is jammed by an abrupt change in conditions into a structure that retains the high disorder of a fluid but acquires the inability to flow that characterizes a solid (25). Although the mechanisms by which either the TC or the supercompressed films would form in the lungs remain unclear, both could explain the metastability implied by the persistently high π .

The temperature dependence of pulmonary mechanics should provide one means of characterizing the surfactant film in situ (4 – 6, 21, 22). When heated at $\pi > \pi_c$, solid films should collapse as soon as they melt to a fluid state, and π should fall to π_c . In the lungs, the higher surface tension would increase the elastic recoil forces, and the hydrostatic pressure required to maintain any particular volume would also increase. TC films of DPPC melt over a narrow range of temperatures (7), and the classical model, therefore, predicts that pulmonary mechanics should change over a similar interval (4 – 6). The studies here determine whether the supercompressed fluid films melt at different temperatures than for TC DPPC so that the temperature dependence of pulmonary mechanics might distinguish which film is present in the lungs.

MATERIALS AND METHODS

Materials

DPPC and 1-palmitoyl-2-oleoyl phosphatidylcholine (POPC) were obtained from Avanti Polar Lipids (Alabaster, AL) and used without further characterization or purification. Extracted calf surfactant [calf lung surfactant extract (CLSE)], obtained by organic extraction of large surfactant aggregates lavaged from calf lungs, was provided by Dr. Edmund Egan of ONY (Amherst, NY). The complete set of neutral and phospholipids (N&PL) was obtained from CLSE by using gel permeation chromatography to remove the hydrophobic proteins (10, 17). The following reagents were purchased commercially and used without further purification: chloroform and methanol (Burdick and Jackson, Muskegon, MI), NaCl (Mallinckrodt Specialty Chemical, Paris, KY), HEPES (Sigma), and $\text{CaCl}_2 \cdot 2\text{H}_2\text{O}$ (J. T. Baker, Phillipsburg, NJ). Agarose was obtained from Sigma (St. Louis, MO) and purified by extraction with organic solvent (3). Water was distilled and then filtered through Macropure, Ultrapure DI and Organic Free Cartridges from Barnstead/Thermolyne Corp (Dubuque, IA). All glassware was acid cleaned.

Methods

Monomolecular films were manipulated on a captive bubble apparatus (32) modified from the original design to allow regulation of the bubble by varying hydrostatic pressure (26). The system uses an air bubble suspended in aqueous buffer below an agarose dome in an inverted spectrophotometric cuvette with a 1-cm path length (7, 33). Temperature is measured with a needle probe (YSI Temperature, Dayton, OH) and controlled by a digital regulator (Cole-Palmer, Vernon Hills, IL) via heating pads (Minco, Minneapolis, MN) applied along the sides of the chamber. A charged-coupled device camera directed along the horizontal axis of the axisymmetric bubble captures the profile via frame grabber to computer, which uses programs in LabVIEW (National Instruments, Austin, TX) to calculate surface area and π . Phospholipid monolayers are formed by spreading small volumes of solutions in chloroform at the air/water interface of the bubble. The studies here used $\sim 0.07 \mu\text{l}$ of solutions containing 4 mM phospholipid. The spreading solvent is removed by exhaustive exchange of the subphase (7). Infusion or withdrawal of subphase by a computer-controlled syringe pump manipulates the bubble to control selected variables in a predetermined fashion (33).

RESULTS

Solid films

We first obtained compression isotherms that confirmed the previously reported phenomena (8, 33, 34), which represent the basis of the present studies (Fig. 1). For monolayers of POPC spread to low initial densities, continuous compression at 23°C produced a monotonic increase in π up to 47 mN/m, after which π changed only slightly during further decreases in area. The roughly isobaric plateau, with π remaining approximately constant, was consistent with the first-order transition observed previously by microscopy in which the LE film collapsed to form a bulk phase (29). In contrast, DPPC monolayers, which passed through the well-known LE-TC coexistence plateau at 7–10 mN/m, showed no discontinuity in the isotherm between 15 and 65 mN/m, indicating the resistance of the TC phase to collapse. Films of POPC also became resistant to collapse if compressed fast enough from ~ 42 mN/m to reach π . The supercompressed POPC films retained their resistance to collapse after completion of the rapid compression, as well as during expansion to $\pi < \pi_e$. During compression at the same rate through the same π at which the original LE film collapsed, π increased steeply for the supercompressed film, with no evidence of collapse.

Monolayers of CLSE generally behaved like POPC (Fig. 1). Compression from large molecular areas produced a monotonic increase in π up to 46 mN/m, with no discontinuity to indicate the coexistence over a broad range of π of the two fluid phases that have been observed microscopically at these nonphysiological temperatures (9, 10). Although the onset of the plateau at ~ 46 mN/m during slow compression was less abrupt than for POPC, the slope of the isotherm decreased greatly at that π , consistent with formation of the previously visualized collapsed phase (29). Rapid compression from $\pi < \pi_e$ to $\pi > 65$ mN/m transformed the film to a persistently metastable structure that resisted collapse, despite return to conditions at which the original monolayer readily collapsed.

Melting at low π

The slope of the isotherm for CLSE during rapid compression, and the difference between the areas at $\pi \approx \pi_e$ before and after rapid compression, both suggested that, during the initial rise of π above π_e , a significant fraction of the constituents in the film left the interface (Fig. 1). The classical model of surfactant function would then explain the resulting metastability of the film after reaching high π by the exclusion of constituents other than DPPC, resulting in a composition sufficiently enriched in DPPC to form the TC phase (1, 6). Previous studies

suggest that such a film would contain essentially pure DPPC (11, 18) and that it would, therefore, have the same melting behavior as a DPPC monolayer.

The first-order transition from the TC to LE phase provides an easily recognized characteristic during melting of DPPC that could be used to determine whether supercompressed CLSE behaved similarly. Heating isobars, obtained by manipulating films to maintain constant π , show the transition for DPPC as an abrupt expansion during the coexistence of the two phases that extend over a narrow range of temperatures (7). Experiments conducted at or below π_c are most easily interpreted because, at higher π , collapse of the film as soon as it forms the LE phase produces a contraction that can obscure the expansion of the TC-LE transition (7). For POPC, the persistent metastability of supercompressed fluid films at $\pi \leq \pi_c$ has allowed heating isobars under conditions at which collapse cannot occur (33). With the films of CLSE, however, after supercompression to high π followed by slow expansion to $\pi < \pi_c$, at which π was held constant, the films showed the isothermal, isobaric expansion (Fig. 2) that our laboratory has observed previously (8). This expansion presumably reflects reinsertion of collapsed constituents facilitated by the surfactant proteins, which are absent in experiments with POPC. Experiments to test whether supercompressed monolayers of CLSE showed the same expansion as TC DPPC were, therefore, confounded by the expansion caused by reinsertion.

Our studies instead used the complete set of N&PL obtained from CLSE to look for the TC-LE transition of DPPC in supercompressed films. Of the several constituents in pulmonary surfactant that promote reinsertion, the hydrophobic surfactant proteins are the most effective (38). After removal of these proteins by gel permeation chromatography, the complete set of N&PL behaved like CLSE in most respects other than reinsertion. Compression of N&PL to high π , like CLSE, produced a decrease in area consistent with exclusion of some constituents and also yielded a metastable film that resisted collapse (Fig. 3). The classical model would again explain the metastability in terms of conversion to a TC film containing only DPPC. Although at 42 mN/m (data not shown), supercompressed N&PL also showed some isothermal expansion consistent with reinsertion, at 44 mN/m (Fig. 3), where the driving force for reinsertion would be less, the area of the film remained constant for the duration of our experiments. As a close substitute for CLSE in which melting would be uncomplicated by reinsertion, we, therefore, obtained heating isobars at 44 mN/m on supercompressed N&PL to determine whether the metastable films were TC DPPC.

During heating of supercompressed N&PL, the films regained the ability to collapse (Fig. 3A). Although at 26°C, slow compression of films after supercompression elevated π above 46 mN/m along a linear isotherm that indicated the absence of collapse (Fig. 3A, yellow line), after heating to 61°C, π reached only 45.4 mN/m and then remained roughly constant during further compression (Fig. 3A, magenta line), consistent with collapse. In the interval over which the films melted, their isobars (Fig. 3B, blue line) showed roughly the same gradual expansion observed for films of N&PL that had been compressed to high π (Fig. 3B, gray line). The abrupt expansion observed during the melting of DPPC (7) was absent. The metastability of supercompressed N&PL, therefore, was unlikely to reflect transformation to a TC film containing only DPPC.

Melting at high π

Heating experiments were then performed to characterize the different metastable films at the high π that occur in the lungs. Films of DPPC, POPC, and CLSE were rapidly compressed from $\pi < 45$ mN/m to 67 ± 2 mN/m, held at that π for 5 min, and then expanded to different π at which heating isobars were obtained. For DPPC, films at $\pi = 45$ mN/m showed the previously reported variation (7), with an initial slow expansion of the TC phase,

followed by the more rapid increase in area that is consistent with TC-LE coexistence (Fig. 4). The coexistence region at 45 mN/m terminated with the change to the lower slope that indicates further expansion of the LE film. This expansion extended to a maximum area at which the slope abruptly fell to negative values, consistent with the collapse of the fluid film. At π above 45 mN/m, this maximum area, which signified the onset of collapse, occurred before completion of the TC-LE coexistence region and at progressively higher temperatures for films at higher π . The steepness of the slope after the onset of collapse varied, with progressively slower contraction at higher π . The π at which area reached its maximum value provided a simple method to characterize the onset of the melting that would be evident in corresponding experiments concerning temperature-dependent changes in pulmonary mechanics (Fig. 4).

Supercompressed films of POPC showed no evidence of the expansion during a first-order transition that occurred for DPPC (Fig. 5). Heating produced the initial slow expansion that previous studies below π_c have shown is comparable to the behavior of POPC monolayers that have not reached high π (33). Films then showed the steeply declining slope of collapse. The variation of the temperature at which contraction began was different for POPC and DPPC. In contrast to DPPC, for which higher π produced higher melting temperatures, collapse was evident for supercompressed POPC earlier at higher π .

Supercompressed films of CLSE, like POPC, showed no evidence of any discontinuous expansion to suggest TC-LE coexistence (Fig. 6). For each isobar, the slope became steeply negative over a narrow range of temperatures. Like DPPC, and in contrast to POPC, the onset of collapse occurred at higher temperatures for heating isobars conducted at higher π (Fig. 7). Melting of CLSE, however, began at temperatures $\sim 10^\circ\text{C}$ lower than for DPPC (Fig. 7).

DISCUSSION

The two kinds of films that can replicate the metastability of pulmonary surfactant observed in the lungs melt at different temperatures. Over the full range of π that occur in situ, films of TC DPPC melt at temperatures at least 10°C higher than for supercompressed CLSE. The different behaviors provide the basis for distinguishing which kind of film more likely represents the structure present in the lungs.

Supercompressed CLSE, however, in one respect behaves more like DPPC than like supercompressed POPC. The melting point for CLSE and DPPC increases at higher π , but POPC shows the opposite trend. The behavior for both DPPC and POPC can be readily explained. For a film melting from a condensed to an expanded phase, the higher π favors the structure with the lower molecular area. Consequently, at higher π , a TC film of DPPC persists to higher temperatures before melting to the LE phase (7). Conversely, for a film such as POPC in which the solid and fluid forms have basically the same structure, any decrease in viscosity that occurs during heating would be apparent earlier at higher π where the thermodynamic driving force for collapse would be greater. This reasoning explains the earlier collapse of POPC at higher π . The tendency for the melting points to increase at higher π is less pronounced for CLSE (Fig. 6) than for DPPC (Fig. 4), but the difference between the behavior for CLSE and POPC (Fig. 5), which in other respects are similar, is somewhat surprising.

The similar π dependence of melting points for DPPC and CLSE raises the possibility that the metastability of the supercompressed mixed lipids reflects formation of a TC film. If, during initial compression, only constituents other than DPPC collapse, the content of that compound might be sufficiently enriched to form the TC phase. The lower melting points

for CLSE than for DPPC would reflect the residual presence of some other constituents and the earlier onset of melting that is commonly seen with the addition of contaminants to a pure compound.

Several considerations make this possibility unlikely, beginning with the similar transformation at high π of supercompressed monolayers containing only POPC (Fig. 1) or dimyristoyl phosphatidylcholine (8), for which a change in composition is impossible. For films containing the complete set of surfactant phospholipids, microscopic studies show that, in the region of phase coexistence below π_c , the TC phase contains essentially pure DPPC (11). The refined film would melt at the same temperatures as spread DPPC rather than at the lower temperatures observed for CLSE. Any TC phase formed by selective exclusion of the coexisting LE phase above π_c should similarly contain only DPPC. Finally, the experiments here show that supercompressed N&PL, which undergoes the same transformation as CLSE to a solid structure at high π , melts to a fluid form with minimal change in area beyond the thermal expansion observed for untransformed N&PL. These results argue that supercompressed CLSE represents a structure other than a TC phase that is greatly enriched in DPPC.

Our results with films of DPPC suggest that the original measurements on the temperature dependence of pulmonary mechanics may have been misinterpreted. The interfacial component of the recoil pressure, obtained by comparing lungs filled with air and with saline, increases abruptly between 35 and 42°C (4 – 6). Because DPPC bilayers melt from the ordered gel phase to the fluid, disordered liquid-crystal phase at 41.4°C (41), the change in pulmonary mechanics suggested an interfacial film that contained only DPPC. The temperature of melting, however, and the point at which collapse becomes rapid (15) depend on π , which is significantly higher in the lungs than in a bilayer. Our results indicate that, if the functional film in situ were TC DPPC, then the change in pulmonary mechanics should occur in the range of 48–55°C, more than 10°C above the experimentally observed values.

The original measurements on the temperature dependence of pulmonary mechanics instead agree closely with the melting behavior of supercompressed CLSE. The temperatures between 36 and 46°C over which the interfacial component of the recoil forces increased for excised rat lungs roughly coincide with the temperatures between 37 and 41°C at which supercompressed CLSE begins to collapse. The results with rat lungs, therefore, suggest that the characteristics of the functional film in situ resemble those of supercompressed CLSE more closely than TC DPPC.

Other groups have subsequently studied the temperature dependence of pulmonary mechanics. Unfortunately, the results at higher temperatures have been conflicting. Studies that extended only up to 37°C have found little change in recoil pressures (16, 24, 40), consistent with the presence of films that melt at higher temperatures. Direct measurements on the surface tension in situ similarly found little difference between 22° and 37°C (31). Studies with cat (20) and rabbit (21, 22) lungs, however, that include measurements at higher temperatures have observed an increase in interfacial recoil pressures that is smaller than for rat lungs and that occurs at significantly higher temperatures, between 42 and 47°C (19, 21, 22). Although the supercompressed fluid and TC films melt at distinct temperatures, the different physiological results prevent any firm conclusion concerning which structure better represents the functional film in the lungs.

Our studies are subject to the major reservation that we have considered only the two kinds of well-defined films that are currently known to replicate the metastability observed in situ. The mechanisms, however, by which either film would form in the lungs remain unknown. The structure of alveolar films could differ from both the supercompressed fluid film and the

highly ordered TC monolayer considered here, and those structural differences might also affect behavior during melting.

Acknowledgments

CLSE was provided by Dr. Edmund Egan of ONY, Inc.

GRANTS

These studies were funded by the National Heart, Lung, and Blood Institute (HL 60914).

References

1. Bangham AD, Morley CJ, Phillips MC. The physical properties of an effective lung surfactant. *Biochim Biophys Acta*. 1979; 573:552–556. [PubMed: 582419]
2. Barber, DJ.; Loudon, R. *An Introduction to the Properties of Condensed Matter*. Cambridge, UK: Cambridge University Press; 1989. p. 21-23.
3. Bligh E, Dyer W. A rapid method of total lipid extraction and purification. *Can J Biochem*. 1959; 37:911–917. [PubMed: 13671378]
4. Clements JA, Trahan HJ. Effect of temperature on pressure-volume characteristics of rat lungs (Abstract). *Fed Proc*. 1963; 22:281.
5. Clements, JA. The alveolar lining layer. In: De Reuck, AVS.; Porter, R., editors. *Development of the Lung*. Boston, MA: Little, Brown; 1967. p. 202-228.
6. Clements JA. Functions of the alveolar lining. *Am Rev Respir Dis*. 1977; 115:67–71. [PubMed: 577382]
7. Crane JM, Putz G, Hall SB. Persistence of phase coexistence in disaturated phosphatidylcholine monolayers at high surface pressures. *Biophys J*. 1999; 77:3134–3143. [PubMed: 10585934]
8. Crane JM, Hall SB. Rapid compression transforms interfacial monolayers of pulmonary surfactant. *Biophys J*. 2001; 80:1863–1872. [PubMed: 11259299]
9. Discher BM, Maloney KM, Schief WR Jr, Grainger DW, Vogel V, Hall SB. Lateral phase separation in interfacial films of pulmonary surfactant. *Biophys J*. 1996; 71:2583–2590. [PubMed: 8913596]
10. Discher BM, Maloney KM, Grainger DW, Sousa CA, Hall SB. Neutral lipids induce critical behavior in interfacial monolayers of pulmonary surfactant. *Biochemistry*. 1999; 38:374–383. [PubMed: 9890919]
11. Discher BM, Schief WR, Vogel V, Hall SB. Phase separation in monolayers of pulmonary surfactant phospholipids at the air-water interface: composition and structure. *Biophys J*. 1999; 77:2051–2061. [PubMed: 10512825]
12. Discher BM, Maloney KM, Grainger DW, Hall SB. Effect of neutral lipids on coexisting phases in monolayers of pulmonary surfactant. *Biophys Chem*. 2002; 101:333–345. [PubMed: 12488012]
13. Fisher MJ, Wilson MF, Weber KC. Determination of alveolar surface area and tension from in situ pressure-volume data. *Respir Physiol*. 1970; 10:159–171. [PubMed: 5505805]
14. Gaines, GL. *Insoluble Monolayers at Liquid-Gas Interfaces*. New York: Interscience; 1966. p. 144-151.
15. Goerke J, Gonzales J. Temperature dependence of dipalmitoyl phosphatidylcholine monolayer stability. *J Appl Physiol*. 1981; 51:1108–1114. [PubMed: 6895370]
16. Gruenwald P. Pulmonary surface forces as affected by temperature. *Arch Pathol*. 1964; 77:568–574. [PubMed: 14130041]
17. Hall SB, Wang Z, Notter RH. Separation of subfractions of the hydrophobic components of calf lung surfactant. *J Lipid Res*. 1994; 35:1386–1394. [PubMed: 7989863]
18. Hildebran JN, Goerke J, Clements JA. Pulmonary surface film stability and composition. *J Appl Physiol*. 1979; 47:604–611. [PubMed: 583282]
19. Horie T, Hildebrandt J. Dynamic compliance, limit cycles, and static equilibria of excised cat lung. *J Appl Physiol*. 1971; 31:423–430. [PubMed: 5111861]

20. Horie T, Ardila R, Hildebrandt J. Static and dynamic properties of excised cat lung in relation to temperature. *J Appl Physiol.* 1974; 36:317–322. [PubMed: 4814300]
21. Inoue H, Inoue C, Hildebrandt J. Temperature and surface forces in excised rabbit lungs. *J Appl Physiol.* 1981; 51:823–829. [PubMed: 7298424]
22. Inoue H, Inoue C, Hildebrandt J. Temperature effects on lung mechanics in air- and liquid-filled rabbit lungs. *J Appl Physiol.* 1982; 53:567–575. [PubMed: 7129978]
23. Kaganer VM, Möhwald H, Dutta P. Structure and phase transitions in Langmuir monolayers. *Rev Mod Phys.* 1999; 71:779–819.
24. Lempert J, Macklem PT. Effect of temperature on rabbit lung surfactant and pressure-volume hysteresis. *J Appl Physiol.* 1971; 31:380–385. [PubMed: 5170908]
25. Liu AJ, Nagel SR. Jamming is not just cool any more. *Nature.* 1998; 396:21–22.
26. Putz G, Goerke J, Schürch S, Clements JA. Evaluation of pressure-driven captive bubble surfactometer. *J Appl Physiol.* 1994; 76:1417–1424. [PubMed: 8045814]
27. Rapp B, Gruler H. Phase transitions in thin smectic films at the air-water interface. *Phys Rev A.* 1990; 42:2215–2218. [PubMed: 9904270]
28. Rugonyi S, Smith EC, Hall SB. Transformation diagrams for the collapse of a phospholipid monolayer. *Langmuir.* 2004; 20:10100–10106. [PubMed: 15518500]
29. Schief WR, Antia M, Discher BM, Hall SB, Vogel V. Liquid-crystalline collapse of pulmonary surfactant monolayers. *Biophys J.* 2003; 84:3792–3806. [PubMed: 12770885]
30. Schürch S. Surface tension at low lung volumes: dependence on time and alveolar size. *Respir Physiol.* 1982; 48:339–355. [PubMed: 7123020]
31. Schürch S, Bachofen H, Weibel ER. Alveolar surface tensions in excised rabbit lungs: effect of temperature. *Respir Physiol.* 1985; 62:31–45. [PubMed: 4070835]
32. Schürch S, Bachofen H, Goerke J, Possmayer F. A captive bubble method reproduces the in situ behavior of lung surfactant monolayers. *J Appl Physiol.* 1989; 67:2389–2396. [PubMed: 2606846]
33. Smith EC, Crane JM, Laderas TG, Hall SB. Metastability of a supercompressed fluid monolayer. *Biophys J.* 2003; 85:3048–3057. [PubMed: 14581205]
34. Smith EC, Laderas TG, Crane JM, Hall SB. Persistence of metastability after expansion of a supercompressed fluid monolayer. *Langmuir.* 2004; 20:4945–4953. [PubMed: 15984255]
35. Smith JC, Stamenovic D. Surface forces in lungs. I. Alveolar surface tension-lung volume relationships. *J Appl Physiol.* 1986; 60:1341–1350. [PubMed: 3754553]
36. Smith R, Tanford C. The critical micelle concentration of L- α -dipalmitoylphosphatidylcholine in water and water-methanol solutions. *J Mol Biol.* 1972; 67:75–83. [PubMed: 5042465]
37. Valberg PA, Brain JD. Lung surface tension and air space dimensions from multiple pressure-volume curves. *J Appl Physiol.* 1977; 43:730–738. [PubMed: 578511]
38. Wang Z, Hall SB, Notter RH. Dynamic surface activity of films of lung surfactant phospholipids, hydrophobic proteins, and neutral lipids. *J Lipid Res.* 1995; 36:1283–1293. [PubMed: 7666006]
39. Wilson TA. Relations among recoil pressure, surface area, and surface tension in the lung. *J Appl Physiol.* 1981; 50:921–930. [PubMed: 7228763]
40. Wohl ME, Turner J, Mead J. Static volume-pressure curves of dog lungs—in vivo and in vitro. *J Appl Physiol.* 1968; 24:348–354. [PubMed: 5640721]
41. Xu H, Huang CH. Scanning calorimetric study of fully hydrated asymmetric phosphatidylcholines with one acyl chain twice as long as the other. *Biochemistry.* 1987; 26:1036–1043. [PubMed: 3567154]

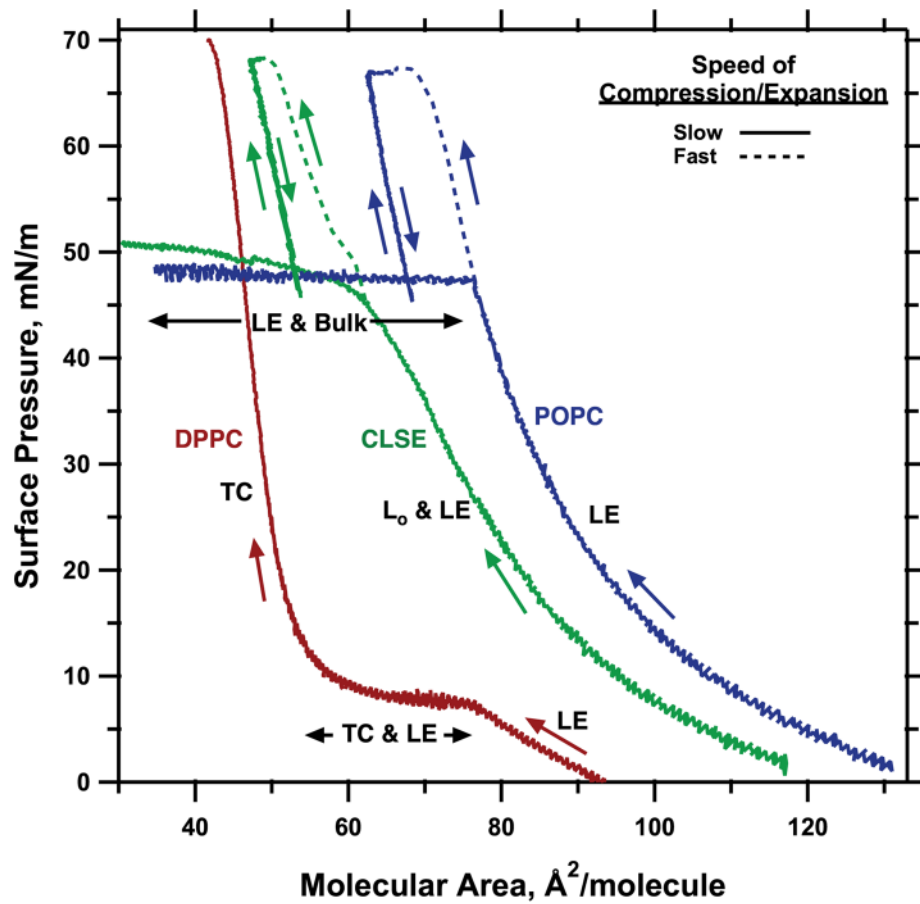


Fig. 1. Compression isotherms illustrating metastable behavior in the three major films studied here. Films spread on a captive bubble at ambient temperatures were compressed either at 23°C [dipalmitoyl phosphatidylcholine (DPPC)] or 26°C [1-palmitoyl-2-oleoyl phosphatidylcholine (POPC); calf lung surfactant extract (CLSE)]. Approximate average rates of change in area were “fast,” $\geq 300 \text{ \AA}^2 \cdot \text{molecule}^{-1} \cdot \text{min}^{-1}$, or “slow,” $\leq 0.8 \text{ \AA}^2 \cdot \text{molecule}^{-1} \cdot \text{min}^{-1}$. Black labels indicate conditions at which previous microscopic studies demonstrate the presence of the tilted-condensed (TC), liquid-expanded (LE), liquid-ordered (L_0), and collapsed bulk phase (9, 10, 12, 29). Colored arrows indicate the direction of progression along the curves.

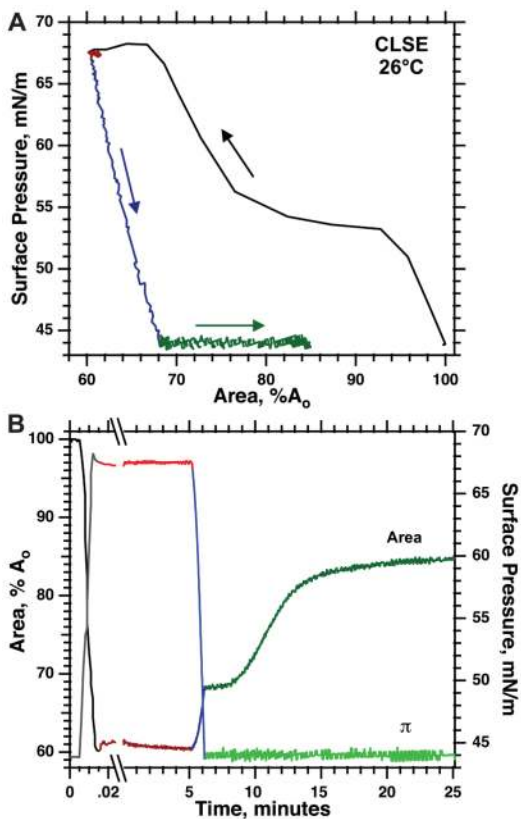


Fig. 2. Isothermal expansion of supercompressed CLSE at surface pressure (π) < equilibrium surface pressure (π_e). Films were spread to 35 mN/m at ambient temperatures and heated to 27.5°C. After slow compression to 44 mN/m (not shown), the films were compressed rapidly to 68 mN/m, held at constant π for 5 min, expanded slowly to 44 mN/m, and then held at that π during isobaric (constant π), isothermal expansion. Area is normalized to the initial value at 44 mN/m (A_0) before the rapid compression. Curves are representative of three experiments. *A*: variation of π with area to clarify the sequence of maneuvers. Arrows indicate the temporal progression of the measurements. *B*: the same data expressed as the variation of π (*right axis*) and area (*left axis*) with time. Split abscissa illustrates the time scale of the initial compression. Colors indicate the same data in the two graphs.

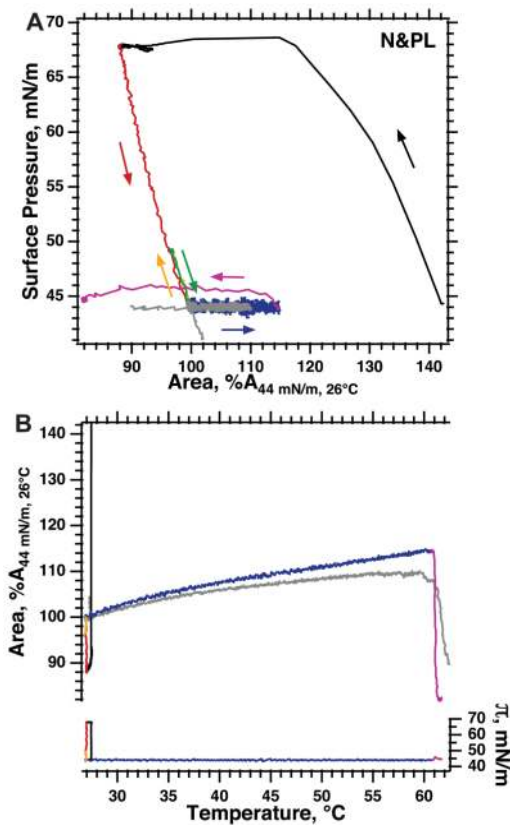


Fig. 3.

Melting of supercompressed neutral and phospholipids (N&PL) at $\pi < \pi_c$. Monolayers of N&PL were spread to an initial π of 35 mN/m at ambient temperatures and heated to 27°C, compressed slowly to 44 mN/m (not shown), then rapidly to 68 mN/m (black curve), followed by expansion to 44 mN/m (red curve). Resistance to collapse was tested by slow compression before (yellow curve) and after (magenta curve) heating films at 1.2°C/min from 27°C to 62.5°C. During heating, the bubble was manipulated using simple feedback to keep the films isobaric (constant π , right axis). In control experiments (gray curve), films were heated isobarically over the same range of temperatures without first undergoing compression to high π . Area is expressed relative to the value at 44 mN/m and 27°C immediately before the onset of heating ($A_{44 \text{ mN/m}, 26^\circ\text{C}}$). Curves are representative of three experiments for both colored and gray curves. *A*: variation of π with area to illustrate the sequence of the maneuvers. Arrows indicate the direction of movement along the curves. *B*: variation of π (right axis) and area (left axis) with temperature. Curves with the same colors in the two panels indicate the same data.

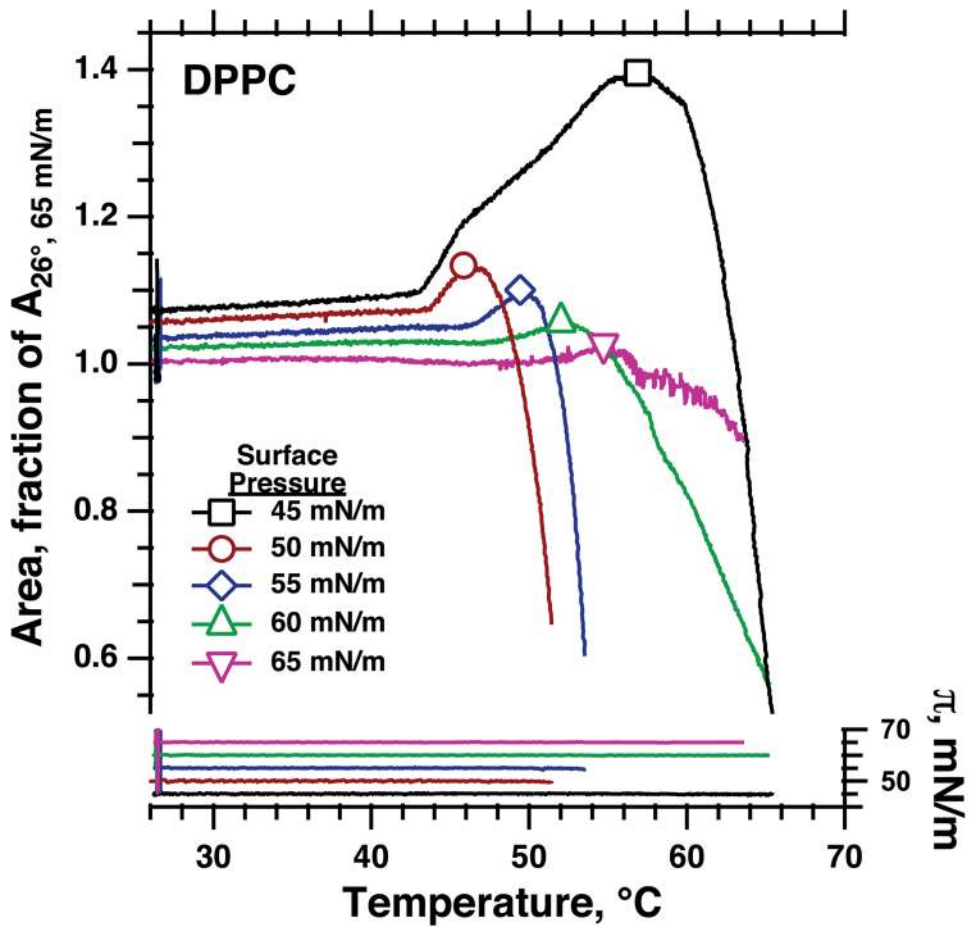


Fig. 4. Melting of DPPC at $\pi > \pi_c$. Films were spread to surface concentrations that produced a $\pi \approx 30$ mN/m at 26.5°C , compressed to $\pi > 65$ mN/m at an average rate of $\sim 300 \text{ \AA}^2 \cdot \text{molecule}^{-1} \cdot \text{min}^{-1}$, and then expanded to the π at which they were heated isobarically (constant π , *right axis*) at $1.2^\circ\text{C}/\text{min}$ until the set π could no longer be maintained. Area is expressed as the fraction of the value at 65 mN/m and 26°C immediately following the initial rapid compression to high π . Curves in each case are representative of three experiments. For each curve, symbols indicate the melting point, defined as the temperature at which area reached its maximum value.

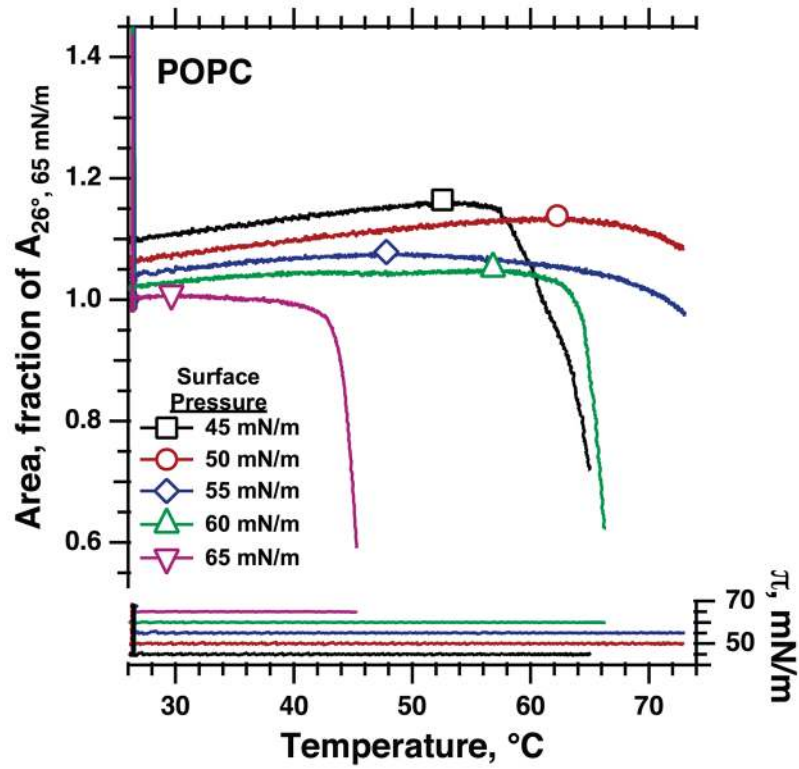


Fig. 5. Melting of supercompressed POPC. Films underwent the same manipulations as DPPC, with initial rapid compression to $\pi > 65 \text{ mN/m}$, followed by expansion to a specific π at which the films were heated isobarically. For each curve, symbols indicate the melting point, defined as the temperature at which area reached its maximum value. Curves are representative of three experiments.

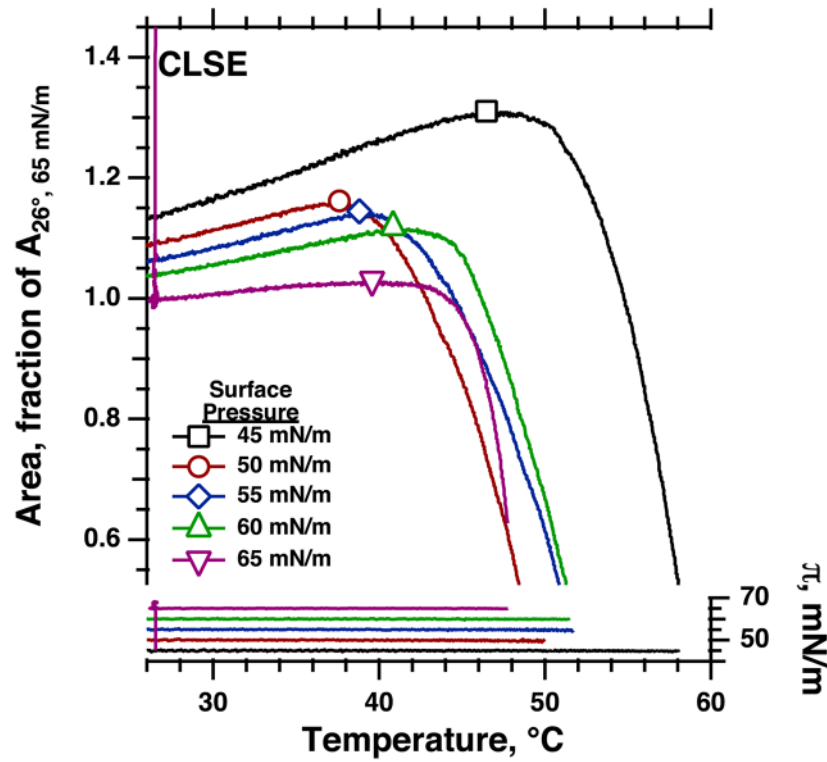


Fig. 6. Melting of supercompressed CLSE. Films were subjected to the same maneuvers as DPPC and POPC, with initial compression to $\pi > 65$ mN/m, followed by expansion to a π at which isobaric heating increased temperature from 26.5°C until the set π could no longer be maintained. Symbols indicate the melting point, defined as the temperature at which area reached its maximum value. Each curve is representative of three experiments.

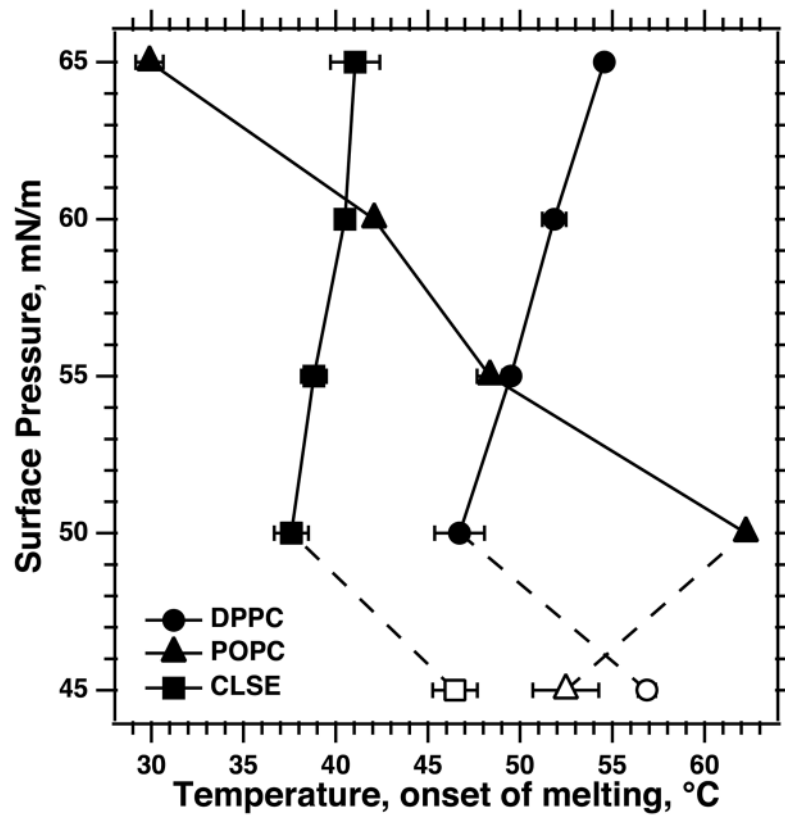


Fig. 7.

Variation of melting points at different π . Symbols give the means \pm SD for melting points obtained as illustrated in Figs. 4 – 6. Open symbols at 45 mN/m indicate the different nature of the change at that π , where, because of the temperature dependence of π_e , the onset of collapse may be unrelated to the solid-to-fluid transition.